



EVALUATION OF NUMERICAL ERRORS IN THE BEM MODELING OF CRACK DYNAMICS: A CASE STUDY

Noriyuki KATSUMATA¹, Ryosuke ANDO², Taku TADA¹ and Yuzo SHINOZAKI¹

SUMMARY

We calculate, with a boundary integral equation method, the field of stress and displacement velocity created by a self-similarly evolving two-dimensional crack in anti-plane shear, and compare the results with known analytic solutions to evaluate the magnitude of numerical errors caused by the discretization. The stress waves, generated by the discontinuous advances of the model crack tips, were found out to have considerably large effects on the numerical solutions, which turned out to be especially serious for the orientation of maximum shear stress. The effects of numerical errors were relatively mild for the amount of slip on the crack.

INTRODUCTION

Numerical simulation studies on the dynamic behavior of earthquake faults in nature tend to entail technical difficulties, as they have to account for the effects of medium inhomogeneities and of the presence of free surfaces. In basic theoretical studies aimed at elucidating the most characteristic properties of fault dynamics, it is therefore a common practice to numerically simulate the dynamic behavior of faults embedded in an elastic medium under more idealized conditions. In doing so, it is unavoidable to discretize the model space with regard to both time and space, so that one should always be aware of the presence of numerical errors coming from the discretization.

In the present study we deal with the problem of a self-similarly evolving anti-plane shear (mode III) crack embedded in an infinite two-dimensional (2-D) medium; we numerically calculate, with a boundary integral equation method (BIEM), the field of stress and displacement velocity created by the crack, and compare the results with known analytic solutions with a view to quantitatively evaluating the magnitude of numerical errors caused by the discretization.

PROBLEM SETTING

Suppose that slip, or displacement discontinuity across a crack, occurs in the y -direction in an infinite,

¹ Department of Architecture, Faculty of Engineering, Tokyo University of Science, Tokyo, Japan. Email: j4103610@ed.kagu.tus.ac.jp (NK), kogutek@rs.kagu.tus.ac.jp (TT), sinozaki@rs.kagu.tus.ac.jp (YS)

² Earthquake Research Institute, The University of Tokyo, Tokyo, Japan. Email: ando@eri.u-tokyo.ac.jp

homogeneous and isotropic medium, in response to an anti-plane shear (mode III) stress $\sigma_{yz} = \sigma_0 (= 1.0)$ operating at infinity, in a 2-D problem setting that does not depend on the y -coordinate. Let a crack emerge at the origin of coordinates at time $t = 0$ and propagate bilaterally along the x -axis at a fixed speed v_r in both $+x$ - and $-x$ -directions (Figure 1). For simplicity, we ignore the effects of friction and assume no stress on the crack surface.

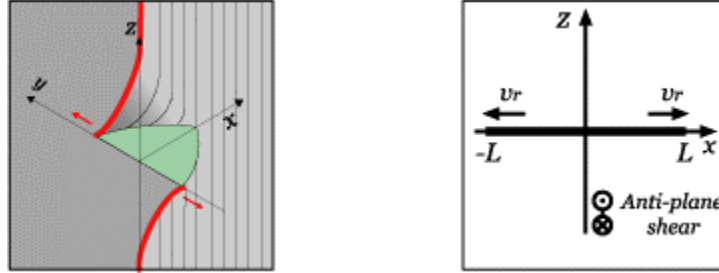


Figure 1. A self-similar two-dimensional anti-plane crack.

The crack problem defined above falls in the category of a self-similar problem, in the sense that it has an invariant form even if you enlarge or reduce both the temporal and spatial scales of the problem by an identical magnification factor. We solve, both analytically and numerically, for the field of stress and displacement velocity created by such a crack and compare both results.

METHOD

The analytical solutions for the stress and displacement velocity field created by a self-similar crack defined above were given by Kostrov [1] and Kikuchi [2]; we numerically evaluated, with Gaussian quadrature, the rigorous expression for the yz -component of stress that is given in the form of an integral on the complex plane.

The numerical solutions for the stress and displacement velocity were calculated with a BIEM scheme, developed by Cochard and Madariaga [3] and expanded by Tada and Madariaga [4], that solves the elastodynamic problem of a planar anti-plane shear crack embedded in a infinite and homogeneous 2-D medium. This method discretizes the crack surface in such a way that the slip rate takes a constant value everywhere within a given spatio-temporal discrete element. As is explained in Tada and Madariaga [4], this numerical technique has two variable parameters associated with the specific method of discretization, namely the Courant-Friedrichs-Lewy (CFL) parameter $h_T = \beta \Delta t / \Delta x$ that gives the ratio of the discrete grid intervals in time and space (β : S-wave speed, Δt : temporal grid interval, Δx : spatial grid interval) and the parameter e_t that defines which position you locate a time collocation point at in a given time grid (the collocation point is located at the end of the corresponding time grid when $e_t = 1.0$ and at the midpoint when $e_t = 0.5$). We used $h_T = 0.5$ and $e_t = 1.0$, the same parameters as used by Cochard and Madariaga [3]. In the following we show all spatial lengths in non-dimensional units as normalized by the crack half-length L , all stress values as normalized by the external stress σ_0 , and all displacement velocities as normalized by $\beta \sigma_0 / \mu$ (where μ is the medium rigidity). The crack tips, which should be advancing continuously at the fixed speed v_r , were modeled as advancing discontinuously by steps of Δx at appropriate time intervals because of the requirement of spatio-temporal discretization.

In the vicinity of the crack, the occurrence of slip on the crack releases shear stress in the direction parallel to it. Cracks generally tend to propagate in the direction that maximizes the shear stress; in fact, for example, the orientation of maximum shear played a major role in Kame and Yamashita's [5] numerical

results that suggested that a crack tends to bend spontaneously when its propagation speed has increased to a certain level. To know the distribution profile of the orientation of maximum shear in the neighborhood of a crack therefore gives a crucial key to the understanding of the dynamic behavior of cracks and of the stress field in their vicinity.

In figures that follow we show distribution profiles for the yx - and yz -components of stress, the (y -component of) displacement velocity, the orientation of maximum shear on the xz -plane and for the amount of slip on the crack surface. The outputs were sampled at grid points spaced at equal intervals of $0.5\Delta x$ in both x - and z -directions so that none falls precisely on the crack surface. Considering spatial symmetry of the problem, we show only the domain corresponding to $x < 0$.

RESULTS

Basic results

Figure 2 shows the analytical solution for the yx - and yz -components of stress, the corresponding numerical solution obtained with the BIEM, as well as the numerical errors defined here as the balance between the two solutions, for the case $L = 24\Delta x$ (entire crack length divided into 48 elements) and $v_r = 0.8\beta$. Propagation of the crack is driven by the yz -component of stress. In both components, the stress is concentrated in the vicinity of the crack tip ($x/L = -1$). As one can see in Figures 2(e) and (f), both stress components are subject to considerably large numerical errors in certain parts of the model plane, the general level of the absolute errors tending to be somewhat higher for the yz - than for the yx -component. One can see arc-shaped zones of large numerical errors that lie at periodic intervals in space. As Ando and Yamashita [6] pointed out, they are thought to be consequences of stress waves that are generated by the discontinuous advances of the tips of the discrete crack model; we will come back to this question in a later section.

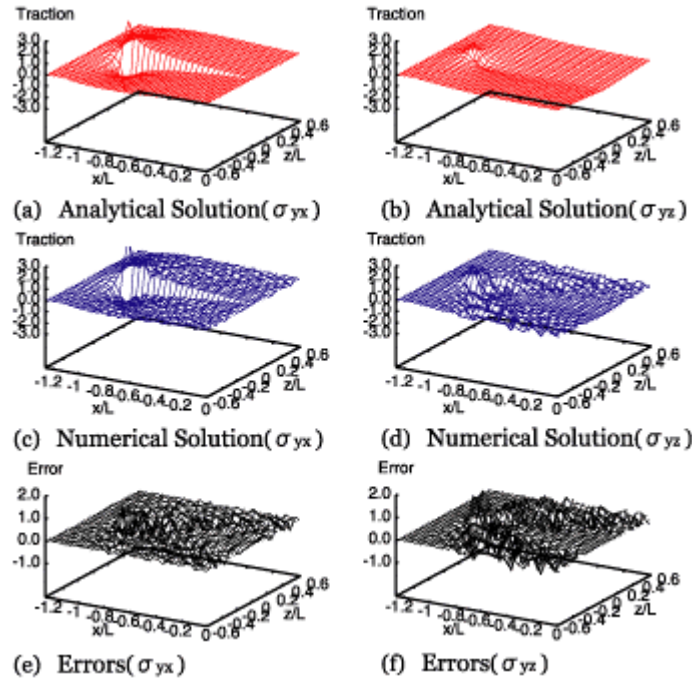


Figure 2. Analytical solutions, numerical solutions and numerical errors for the yx - and yz -components of stress ($L = 24\Delta x$, $v_r = 0.8\beta$).

Figure 3 shows the analytical solution, numerical solution and numerical errors in the same case for the y -component of displacement velocity; one can recognize zones of large numerical errors just as in the case of the stress components. Incidentally speaking, the relative numerical errors, which we define as the absolute numerical errors (Figure 3(c)) divided by the analytic solution, had approximately the same levels of magnitude for the displacement velocity and for the yz -component of stress.

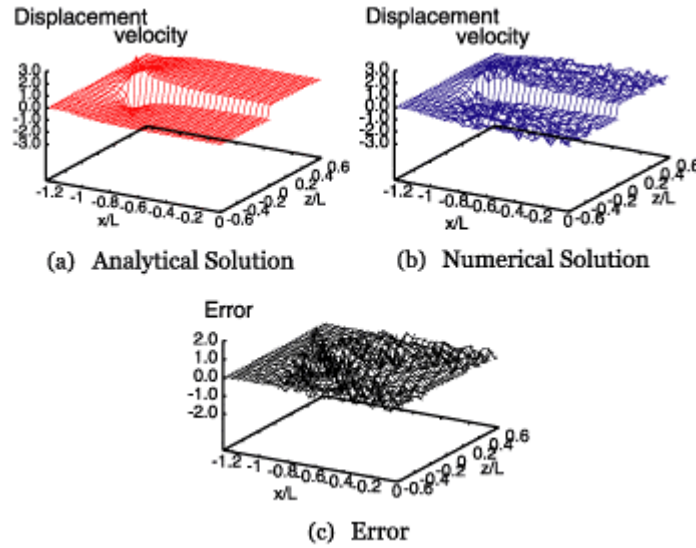


Figure 3. Analytical solution, numerical solution and numerical errors for the displacement velocity ($L = 24\Delta x$, $\nu_r = 0.8\beta$).

Figure 4 shows, with line segments, the orientation of maximum shear calculated for each grid point using the magnitudes of the yx - and yz -components of stress in both the analytic and numerical solutions:

$$\theta = \arctan (-\sigma_{yx}/\sigma_{yz}), \quad (1)$$

where θ is the angle measured counterclockwise from the x -axis. Waves generated by slip on the crack disturbs the initial, homogeneous field of stress and, on and in the vicinity of the crack, releases shear stress in the direction parallel to it; this explains why the orientation of maximum shear is nearly perpendicular to the crack in its vicinity. Reflecting the numerical errors in the individual stress components, the calculated orientation of maximum shear has discrepant distribution patterns for the analytical and numerical solutions. The discrepancies are particularly serious within arc-shaped zones that lie at periodic intervals in space; as we have said above, these are thought to be related to stress waves generated at the tips of the discrete crack model. The blank parts in the top left and bottom left corners of the panels represent zones of undisturbed initial stress where the waves have not arrived yet.

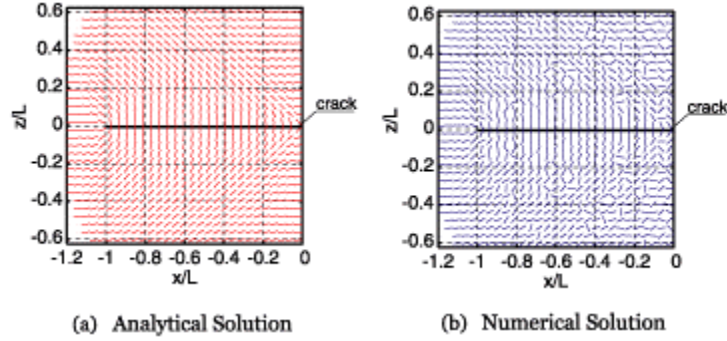


Figure 4. Analytical and numerical solutions for the orientation of maximum shear stress ($L = 24\Delta x$, $v_r = 0.8\beta$).

Figure 5 shows the analytical solution, numerical solution and numerical errors in the same case for the amount of slip on the crack surface; slip is larger in the numerical solution than in the analytical, since the numerical scheme tends to evaluate, in the vicinity of the crack tips ($|x/L| = 1$), the slip rate to be larger than what it is in the analytical solution. Figure 5(b) shows that large absolute values of numerical errors appear only near the tips of the crack ($0.8 < |x/L| = 1$). As for the relative numerical errors, they tended to be smaller for the amount of slip than for the stress components.

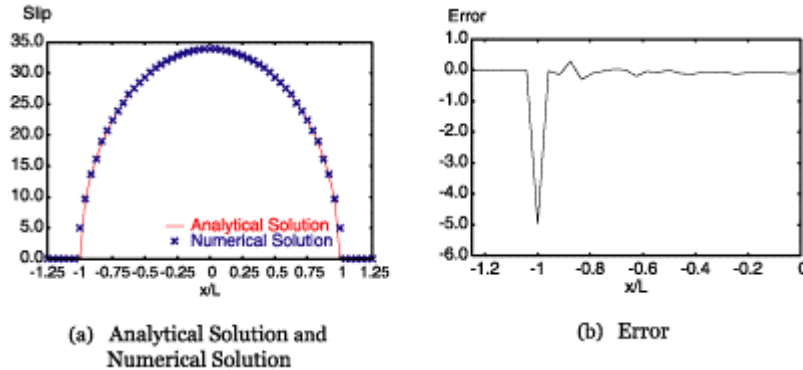


Figure 5. Analytical solutions, numerical solutions and numerical errors for the amount of slip on the crack surface ($L = 24\Delta x$, $v_r = 0.8\beta$).

Dependency on the propagation speed

Figure 6 shows how the numerical precision changes for the stress components when we fix the number of crack divisions at 48 ($L = 24\Delta x$) and alter the speed v_r of crack propagation; the results for $v_r = 0.5\beta$ and $v_r = 0.8\beta$ are given as the most representative cases. Plotted are the analytical solution, numerical solution, and numerical errors defined as their balance, for the individual stress components on the rows of grid points along the lines $|z/L| = 1/96$ that are parallel to the x -axis and lie the closest to the crack plane. As one can see in Figures 6(e) and (f), the numerical errors for the yx -component of stress were generally larger near the central part of the crack ($|x/L| = 0.8$) when $v_r = 0.5\beta$ than when $v_r = 0.8\beta$, but no similar characteristic differences were recognized for the yz -component of stress.

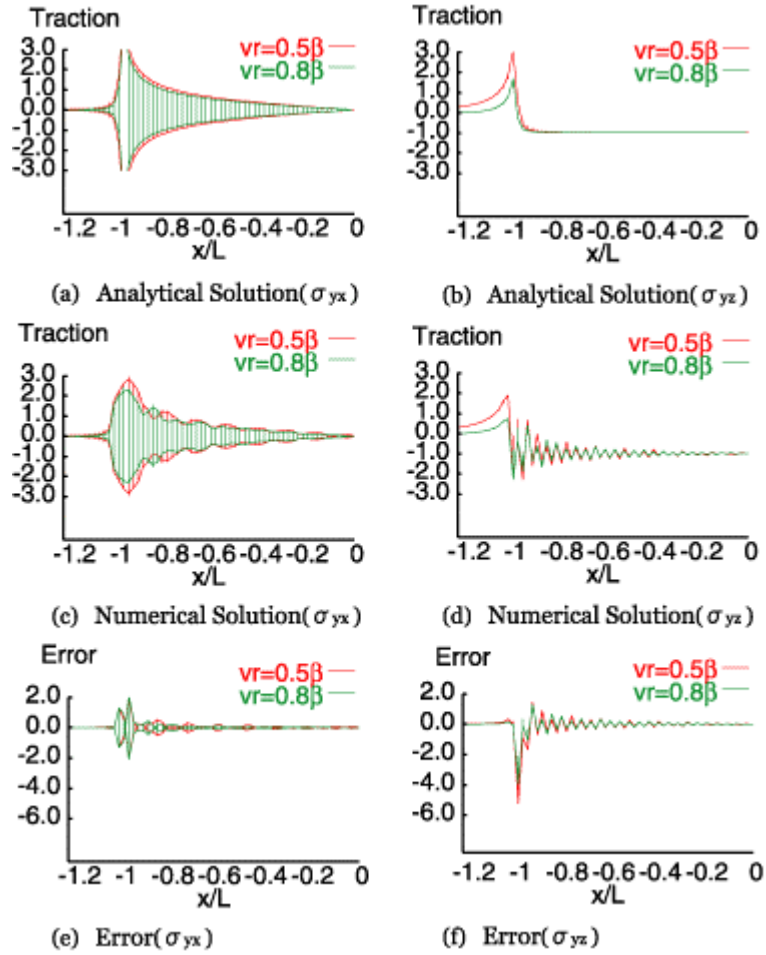


Figure 6. Analytical solutions, numerical solutions and numerical errors for the yx - and yz -components of stress on the rows of grid points parallel to the x -axis and lying close to the crack plane, for two different values of the crack propagation speed ($L = 24\Delta x$, $|z/L| = 1/96$).

Figure 7 shows changes in numerical errors for the displacement velocity in the close vicinity of the crack plane in the same situation. The numerical errors tended to be slightly larger for the case of $v_r = 0.5\beta$ than for $v_r = 0.8\beta$, but no characteristic differences were found in the pattern of their appearance.

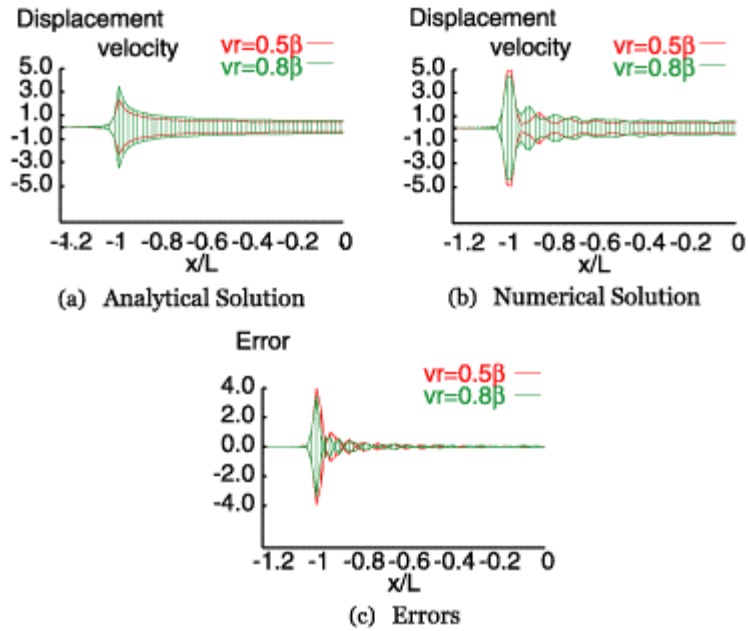


Figure 7. Analytical solution, numerical solution and numerical errors for the displacement velocity on the rows of grid points parallel to the x -axis and lying close to the crack plane, for two different values of the crack propagation speed ($L = 24\Delta x$, $|z/L| = 1/96$).

Figure 8 shows the numerical solution for the orientation of maximum shear stress for the case of $v_r = 0.5\beta$ with the number of crack divisions fixed at 48. One can see that the stress waves thought to have emanated from the crack tips (zones of conspicuously large discrepancies between the analytically and numerically obtained orientations of maximum shear) are spaced at larger intervals than in the case of $v_r = 0.8\beta$; this reflects the fact that the crack tips advance discontinuously at larger time intervals.

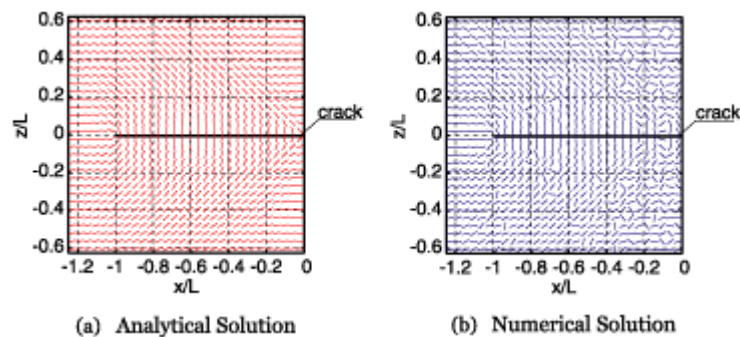


Figure 8. Analytical and numerical solutions for the orientation of maximum shear stress ($L = 24\Delta x$, $v_r = 0.5\beta$).

Figure 9 shows how the numerical precision changes for the amount of slip on the crack surface in the same situation. The numerical errors are generally larger for the case of $v_r = 0.5\beta$ than for $v_r = 0.8\beta$. In both cases, the largest numerical errors are concentrated near the tip of the crack.

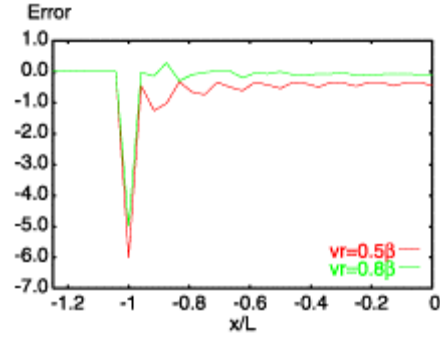


Figure 9. Numerical errors for the amount of slip on the crack surface, for two different values of the crack propagation speed ($L = 24\Delta x$).

Dependency on the number of crack divisions

Figure 10 shows how the numerical precision changes for the stress components when we fix the crack propagation speed at 0.8 times the S wave speed ($v_r = 0.8\beta$) and alter the number of discrete elements constituting the crack; the results for 24, 120 and 240 divisions are shown as the most representative cases. As in the foregoing section, we have plotted the analytical solution, numerical solution, and numerical errors defined as their balance, for the individual stress components on the rows of grid points along the lines $|z/L| = 1/96$ that are parallel to the x -axis and lie the closest to the crack plane. As one can see in Figures 10(e) and (f), numerical precision remarkably improved for both stress components when we increased the number of crack divisions, despite the increasing number of stress waves expected to emanate from the crack tips. When the crack was divided into 120 or 240 elements, in particular, large numerical errors appeared only near the tips of the crack ($0.8 < |x/L| = 1$). Numerical errors stayed within a range of $\pm 0.15\sigma_0$ for the yx -component of stress and within $\pm 0.03\sigma_0$ for the yz -component near the central part of the crack ($|x/L| = 0.8$) when the number of divisions was 240.

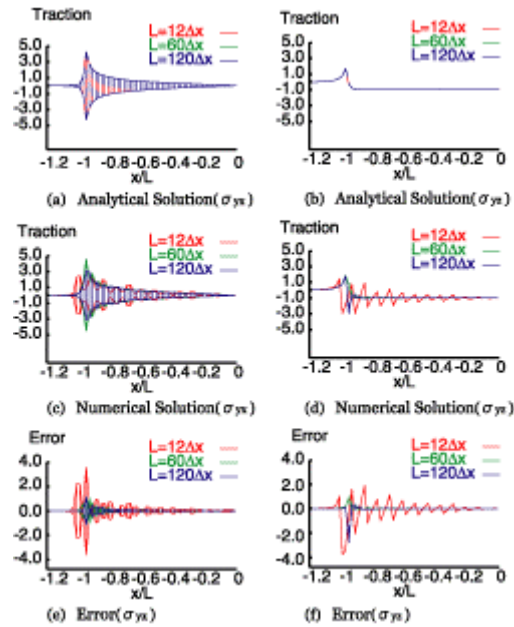


Figure 10. Analytical solutions, numerical solutions and numerical errors for the yx - and yz -components of stress on the rows of grid points parallel to the x -axis and lying close to the crack plane, for three different numbers of crack divisions ($|z/L| = 1/96$, $v_r = 0.8\beta$).

Figure 11 shows changes in numerical errors for the displacement velocity in the close vicinity of the crack plane in the same situation. Just as it did so for the stress components, numerical precision improved when we increased the number of discrete crack elements. The profile of stress concentration near the crack tips ($x/L = 1$) sharpened with the increasing number of crack divisions. When the crack was divided into 120 or 240 elements, large numerical errors appeared only near the tips of the crack ($0.8 < x/L = 1$). Numerical errors stayed within a range of $\pm 0.15\beta\sigma_0/\mu$ near the central part of the crack ($x/L = 0.8$) when the number of divisions was 240.

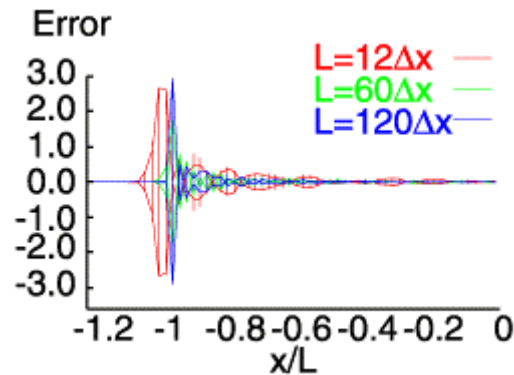


Figure 11. Numerical errors for the displacement velocity on the rows of grid points parallel to the x -axis and lying close to the crack plane, for three different numbers of crack divisions ($z/L = 1/96$, $v_r = 0.8\beta$).

Figure 12 shows the numerical solution for the orientation of maximum shear for the case of 240 crack divisions ($L = 120\Delta x$) with the crack propagation speed fixed at $v_r = 0.8\beta$. Despite the improved numerical precision for the individual stress components, the disarranged distribution profile of the orientation of maximum shear shows no recognizable improvement, because of the local effects of the stress waves emanating from the crack tips. This can be understood by recalling the fact that the orientation of maximum shear is determined by the ratio of the individual stress components (Equation (1)).

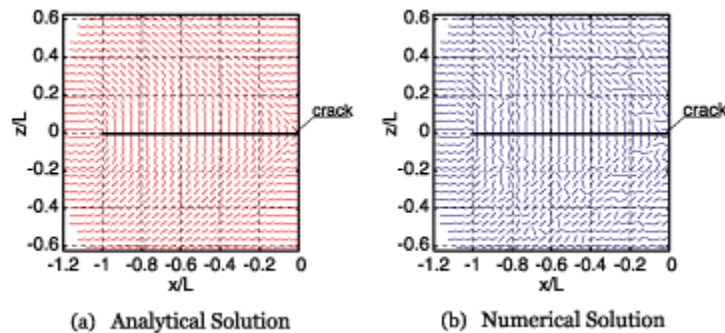


Figure 12. Analytical and numerical solutions for the orientation of maximum shear stress ($L = 120\Delta x$, $v_r = 0.8\beta$).

Figure 13 shows how the numerical precision changes for the amount of slip on the crack surface in the same situation. The numerical errors tended to increase near the crack tips ($0.8 < x/L = 1$) but reduced slightly in the central part of the crack ($x/L = 0.6$) with the increasing number of crack divisions.

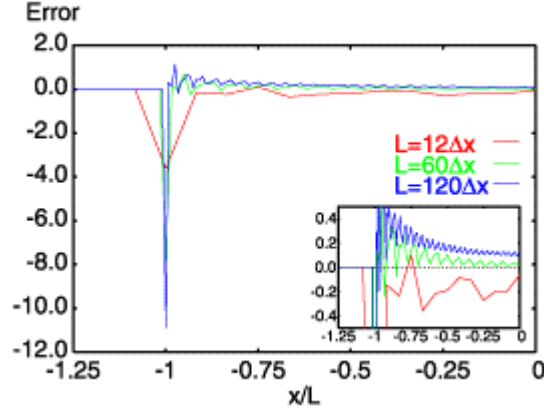


Figure 13. Numerical errors for the amount of slip on the crack surface, for three different numbers of crack divisions ($v_r = 0.8\beta$).

Some discussions on the effects of stress waves

As we have said in a foregoing section, it is thought to be due to the effects of stress waves, emanating from the tips of the discrete model crack that advance discontinuously, that zones of large numerical errors emerge at periodic intervals in space in 2-D distribution profile maps for the stress and displacement velocity outside the crack. With a view to bearing out this hypothetical interpretation, we have conducted a simple numerical test to compare two different types of model cracks, one with a tip that advances smoothly and the other with a tip that advances discontinuously.

Consider a 2-D anti-plane crack that emerges at the origin of the xz -coordinate system at time $t=0$ and propagates unilaterally along the $+x$ -axis at a fixed speed of v_r , with the amount of slip fixed at unity everywhere within the crack (Figure 14(a)). The mechanical conditions imposed on the interior of the crack are thus completely different than in the numerical tests heretofore described). The field of stress and displacement velocity created by such a crack, which is known as a Haskell model, can be obtained analytically with the Cagniard-de Hoop method. We also numerically analyze this Haskell model crack with Tada and Madariaga's [4] method through spatio-temporal discretization, assuming the crack tip to advance discontinuously; we place, at the crack front, a discrete element within which the slip velocity takes a finite and constant value, and set the slip velocity at zero everywhere except within that crack front element (Figure 14(b)).

Figures 14(c)-(f) show the analytical and numerical solutions for the y_x - and y_z -components of stress for the case where the crack propagation velocity $v_r = (2/3)\beta$, the grid parameter $h_T = 1/3$, the time collocation parameter $e_t = 1.0$ and the crack is divided into 24 elements ($L = 24\Delta x$). In either stress component, only in the model with the discontinuously advancing crack tip did zones of large numerical errors appear at periodic intervals in space, and they had arc-like shapes centered near the tip of the crack. This observation gives another proof that the similar zones of large numerical errors, which emerged at periodic intervals in space in the numerical solutions for self-similar crack problems, were related to stress waves that emanated from the crack tips modeled as advancing discontinuously because of the requirement of discretization.

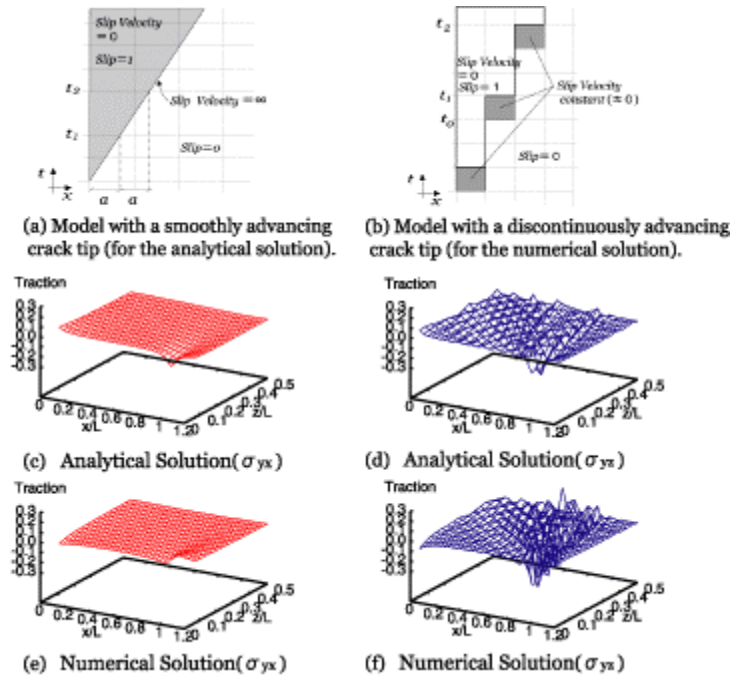


Figure 14. Analytical and numerical solutions for the stress field created by a Haskell fault model ($L = 24\Delta x$, $v_r = (2/3)\beta$).

CONCLUSION

In the present study we have calculated, with a BIEM, the field of stress and displacement velocity created by a self-similar 2-D anti-plane crack as well as the amount of slip on its surface and, by comparing the results with known analytical solutions, evaluated the magnitude of numerical errors due to the discretization as well as the profile of their distribution in space. It was revealed that the numerical solutions for the field of stress and displacement velocity outside the crack were, depending on the location on the model space, subject to considerably large effects of the stress waves that emanate from the crack tips which are modeled as advancing discontinuously because of the requirement of the discretization. The effects of numerical errors were particularly serious on the orientation of maximum shear that is calculated at each sample point from the magnitudes of individual stress components, a reminder that we should not be too careful of the effects of numerical errors in conducting numerical calculations where the orientation of maximum shear comes into play, such as in the simulation of spontaneous crack growth. On the other hand, the effects of numerical errors were relatively mind for the amount of slip on the crack surface except in the vicinity of its tips.

Within the scope of the present study, the numerical errors did not show characteristic changes in magnitude and spatial distribution profile when we varied the crack propagation speed, but numerical precision was remarkably improved when we refined the grid size and increased the number of crack divisions. In the latter case, however, the seriously disarranged distribution profile of the orientation of maximum shear hardly showed any recognizable improvement, in spite of the improved numerical precision for the individual stress components, because of the strong local effects of the stress waves.

Insights obtained from the present study are expected to provide implications to a number of related research subjects, since numerical methods of the same category are widely in use to deal with the cases of 2-D in-plane, 3-D and non-planar crack problems.

REFERENCES

1. Kostrov BV. "Selfsimilar problems of propagation of shear cracks." *PMM Journal of Applied Mathematics and Mechanics* 1964; 28: 1077-87.
2. Kikuchi M. "Displacement velocity and stress fields caused by a two-dimensional self-similar crack (in Japanese with English abstract)." *Zisin Journal of the Seismological Society of Japan , Second Series*, 1976; 29(3): 277-85.
3. Cochard A, Madariaga R. "Dynamic faulting under rate-dependent friction." *Pure and Applied Geophysics* 1994; 142(3/4): 419-45.
4. Tada T, Madariaga R. "Dynamic modelling of the flat 2-D crack by a semi-analytic BIEM scheme." *International Journal for Numerical Methods in Engineering* 2001; 50(1): 227-51.
5. Kame N, Yamashita T. "Simulation of the spontaneous growth of a dynamic crack without constraints on the crack tip path." *Geophysical Journal International* 1999; 139(2): 345-58.
6. Ando R, Yamashita T. "Dynamic interactions between fault segments and the formation of fault system (in Japanese with English abstract)." *Zisin, Journal of the Seismological Society of Japan, Second Series* 2003; 56(1): 1-9.